

## Multiple membrane cavity optomechanics

M. Bhattacharya and P. Meystre

B2 Institute, Department of Physics and College of Optical Sciences, The University of Arizona, Tucson, Arizona 85721, USA

(Received 8 April 2008; published 1 October 2008)

We investigate theoretically the extension of cavity optomechanics to multiple membrane systems. We describe the simplest case of two membranes in a cavity, in terms of the coupling of the light fields to the breathing and center-of-mass modes of the membrane array. We show that these normal modes can be optically addressed individually and also be cooled, trapped, and characterized, e.g., via quantum nondemolition measurements. The extension to a larger number of membranes is briefly discussed.

DOI: [10.1103/PhysRevA.78.041801](https://doi.org/10.1103/PhysRevA.78.041801)

PACS number(s): 42.50.Pq, 03.67.Lx, 42.65.Sf, 85.85.+j

Cavity optomechanics is an emerging field at the boundary between quantum optics and nanoscience. Resulting in part from experimental innovations at the mesoscopic scale, optomechanical systems—mechanical systems that can be manipulated by light—have recently generated much experimental and theoretical interest [1–6]. They offer the prospect of realizing quantum effects at a macroscopic scale [7], of supplying quantum sensors for applications ranging from single molecule detection [8] to gravitational wave interferometry [6,9], for the quantum control of atomic, molecular, and optical systems [10], and for possible new quantum information processing devices [11].

As cavity optomechanics begins to mature as a field, we recognize that scalability is an important aspect of any technology. In particular, it is immediately relevant to possible uses in information processing. This has been acknowledged in proposals for constructing quantum computers using trapped ions, cavity quantum electrodynamics, neutral-atomic lattices, nuclear magnetic resonance, spintronics, dipolar molecules, etc.; see Ref. [12] and references therein. It is therefore important to investigate the scaling of current cavity-based techniques to a larger number of optomechanical elements.

In this Rapid Communication, motivated by a pioneering experiment with one membrane [13], we consider the optomechanical cooling and trapping of two partially transparent dielectric membranes inside a high-finesse cavity driven by laser radiation (Fig. 1). Presenting both exact numerical as well as approximate analytical results, we show that such a system is described most conveniently in terms of the *normal modes* of the linear chain formed by the membranes. Further, we demonstrate that these mechanical modes can be optically addressed individually, and their cooling, trapping, and measurement are feasible. We conclude by briefly addressing the case of a larger array of membranes.

Our starting point is a cavity with two fixed and perfectly reflecting end mirrors and two identical vibrating nonabsorptive dielectric membranes, each of reflectivity  $R$ , mass  $m$ , and mechanical frequency  $\omega_m$ ; see Fig. 1. We begin by calculating the cavity mode frequencies. Their dependence on the positions  $q_{1,2}$  of the membranes is central to the description of the system, as it determines the optomechanical couplings [14]. For  $R=1$ , the resonator consists simply of three uncoupled cavities whose eigenfrequencies in the absence of membrane motion ( $q_{1,2}=\mp L$ ) are threefold degenerate and are given by

$$\omega_n = \frac{n\pi c}{2L}. \quad (1)$$

Here  $n$  is a positive integer,  $c$  is the velocity of light, and  $2L$  is the length of each subcavity.

For  $R \neq 1$ , the three resonators are coupled, and this coupling lifts the degeneracy of the frequencies  $\omega_n$ . We assume that the moving membranes are much thinner than an optical wavelength; modeling them by spatial  $\delta$  functions allows us to write the electric susceptibility inside the full resonator as [15]

$$\epsilon(x) = \epsilon_0 \left( 1 + \frac{\eta}{k} [\delta(x - q_1) + \delta(x - q_2)] \right), \quad (2)$$

where  $\epsilon_0$  is the dielectric permittivity of vacuum,  $\eta = 2\sqrt{R/(1-R)}$ , and  $k$  is the wave number of light. The intracavity electric field, which vanishes at  $x = \pm 3L$ , is given by

$$E(x) = \begin{cases} E_1 \sin k(x + 3L), & -3L \leq x \leq q_1, \\ E_2 \sin kx + E_3 \cos kx, & q_1 \leq x \leq q_2, \\ E_4 \sin k(x - 3L), & q_2 \leq x \leq 3L, \end{cases} \quad (3)$$

where  $E_{1,2,3,4}$  are constants. These constants can be eliminated by exploiting the continuity of  $E(x)$  at  $x=q_{1,2}$  and integrating the Helmholtz wave equation  $d^2E(x)/dx^2 = -\mu_0\epsilon(x)E(x)$  across the discontinuities in Eq. (2),  $\mu_0$  being

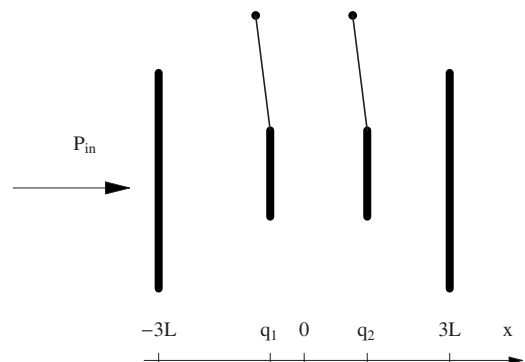


FIG. 1. A high-finesse optical cavity with two mirrors fixed at  $\pm 3L$ , and two dielectric membranes centered at  $q_1 \sim -L$  and  $q_2 \sim L$ , respectively.  $P_{in}$  signifies the power of the laser radiation that may be used to drive the cavity.

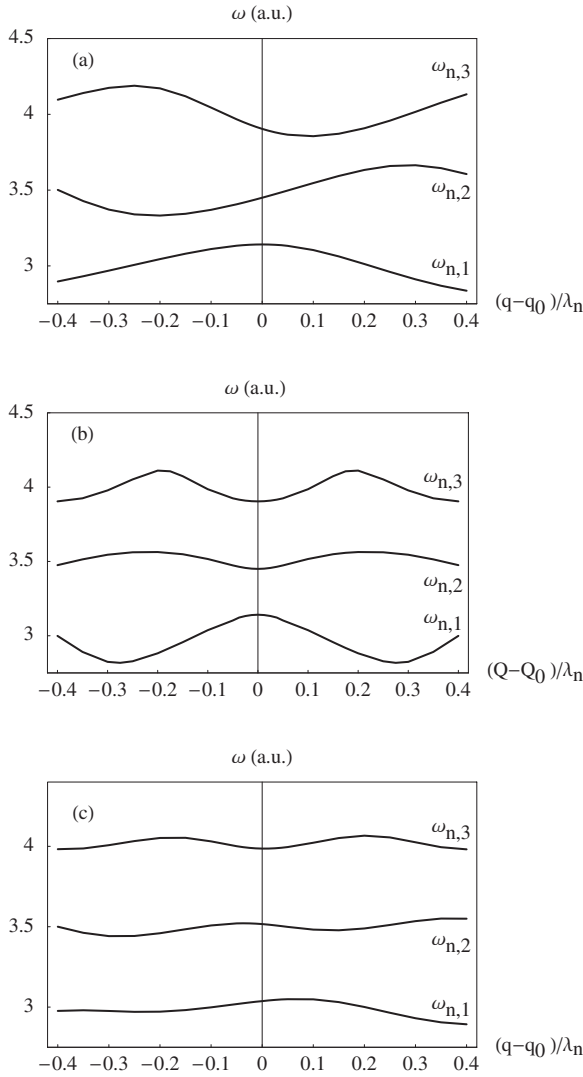


FIG. 2. Generic portion of the optical frequency spectrum for the two-membrane cavity shown as a function of the membrane normal coordinates  $q-q_0$  and  $Q-Q_0$  each scaled by the wavelength  $\lambda_n=4L/n$ . The curves correspond to numerical solutions of Eq. (4). A closely spaced triplet of frequencies  $\omega_{n,i}$  ( $i=1,2,3$ ) is shown in (a) as a function of  $q$  about  $q_0=2L$ ,  $Q_0=0$ , in (b) as a function of  $Q$  about  $q_0=2L$ ,  $Q_0=0$ , and in (c) as a function of  $q$  about  $q_0=2L$ ,  $Q_0=0.12\lambda_n$ . The cavity parameters used in the plot are  $R=0.7$ ,  $L=10$  cm,  $n=10^5$ , similar to the experiment of Ref. [13].

the magnetic permeability of vacuum. Doing so yields a trigonometric equation governing the allowed values of  $k$ , i.e., the spectrum,

$$\begin{aligned} & \sin 2(\theta + 3kL) + \sin^2 \theta \sin 2k(3L - q) \\ & = 2 \sin \theta \cos(\theta + kq) \cos 2kQ, \end{aligned} \quad (4)$$

where  $\sin \theta = \sqrt{R}$ ,  $q = q_1 - q_2$  is the relative coordinate, and  $Q = (q_1 + q_2)/2$  is the center-of-mass (COM) coordinate of the oscillating membranes. We note that the effective masses and frequencies of the relative and COM modes are  $m/2, 2m$  and  $\omega_m \sqrt{3}, \omega_m$ , respectively [16].

The numerical solution of Eq. (4) for a given set of system parameters produces an involved three-dimensional plot

of the spectrum as a function of the coordinates  $q$  and  $Q$ . To simplify the discussion below, we have chosen to display generic two-dimensional sections showing a closely spaced frequency triplet in Fig. 2. The optical frequencies show strong modulations along both  $q$  and  $Q$ . They arise from the avoided crossings associated with the lifting of the degeneracy of the frequency triplet due to the coupling of the subcavities.

Considerable insight can be gained from approximate analytical solutions of Eq. (4). Perturbation theory in the small parameters  $(q-q_0)/\lambda$  and  $(Q-Q_0)/\lambda \sim 10^{-5}$  [24], where  $\lambda$  is the optical wavelength yields, for example, the triplet ( $i=1,2,3$ ) of optical frequencies in the vicinity of any  $q_0$  and  $Q_0$ ,

$$\begin{aligned} \omega_{n,i}(q, Q) = & \Delta_{n,i} + B_{n,i}(q - q_0) + B'_{n,i}(Q - Q_0) + M_{n,i}(q - q_0)^2 \\ & + M'_{n,i}(Q - Q_0)^2 + P_{n,i}(q - q_0)(Q - Q_0) + \dots \end{aligned} \quad (5)$$

The various terms in this equation fully describe the basic optomechanical properties of the system. Specifically,  $\Delta_{n,i}$  includes the frequency shifts due to the subresonators coupling in the absence of membrane motion;  $B_{n,i}$  and  $B'_{n,i}$  determine the strength of the linear optomechanical couplings associated with the “breathing” and COM modes of motion, respectively, producing a backaction of the mirror motion on the light field that can be exploited in mirror cooling; and  $M_{n,i}$  and  $M'_{n,i}$  govern the quadratic couplings that may lead to quantum nondemolition (QND) energy measurements [13]. Finally  $P_{n,i}$  quantifies the coupling between the relative and COM modes and is responsible for normal mode decoherence as well as down conversion [17].

Combining our numerical and analytical considerations we now show how each mechanical mode can be independently accessed optically. First we consider backaction effects on  $q$ . We arrange the membranes so that  $q_0=2L$ , and  $Q_0=0$  [Figs. 2(a) and 2(b)], and consider the frequency of the mode  $\omega_{n,2}$  at that position. The shift in that case is given by

$$\Delta_{n,2} = \omega_n + \frac{c}{2L} \left[ \sin^{-1} \left( \frac{\sqrt{3 + \sin^2 \theta}}{2} \right) - \theta \right]. \quad (6)$$

Taking the parameters  $R=0.7$ ,  $L \sim 10$  cm, and  $n \sim 10^5$  from the experiment of Ref. [13] we find  $\omega_n \sim 10^{15}$  Hz, the remainder of the shift in Eq. (6) being 0.5 GHz. The slope along  $q$  turns out to be

$$B_{n,2} = \frac{\xi_{n,2} \sin 2\theta \sin \theta_{n,2}}{3 \sin^2 \theta \cos \theta_{n,2} + 3 \cos(2\theta + 3\theta_{n,2}) + \sin 2\theta \sin \theta_{n,2}},$$

where  $\theta_{n,2} = 2\Delta_{n,2}L/c$  and  $\xi_{n,2} = \Delta_{n,2}/2L$ . For the cavity parameters quoted above,  $B_{n,2} \sim \xi_{n,2}/4$ , similar to that considered in past experiments [1–4,13]. The curvature of  $\omega_{n,2}$  along  $q$  is

$$M_{n,2} = \frac{9B_{n,2}^2 \sin(2\theta + 3\theta_{n,2}) + [3(B_{n,2}^2 + 2\xi_{n,2}^2)\sin\theta - 4B_{n,2} \cos\theta]\sin\theta \sin\theta_{n,2} - (\xi_{n,2} + B_{n,2})^2 \sin 2\theta \cos\theta_{n,2}}{\frac{c}{L}[3 \sin^2\theta \cos\theta_{n,2} + 3 \cos(2\theta + 3\theta_{n,2}) + \sin 2\theta \sin\theta_{n,2}]} \quad (7)$$

which produces a change of the order of 1 Hz in the frequency of that mode. This value is much smaller than the cavity linewidth  $\gamma \sim 10$  MHz [13] and hence can be ignored. This is reflected in Fig. 2(a) where the curvature of  $\omega_{n,2}$  is negligible at  $q_0 = 2L$ .

Clearly, the slope along  $Q$  is  $B'_{n,2} = 0$  since  $\omega_{n,2}$  has a minimum at  $Q_0 = 0$  [Fig. 2(b)]. Also the corresponding curvature is

$$M'_{n,2} = \frac{(4\Delta_{n,2}^3/c^2)\sin\theta \sin(\theta + \theta_{n,2})}{3 \cos(2\theta + 3\theta_{n,2}) + \sin\theta[\sin\theta \cos\theta_{n,2} + 2 \sin(\theta + \theta_{n,2})]}.$$

For the parameters quoted below Eq. (6),  $M'_{n,2} \sim 100$  kHz. Again this is a small fraction of the cavity linewidth, and hence it is negligible. Finally  $P_{n,2} = 0$  since  $\omega_{n,2}$  is symmetric in  $Q$  around  $Q_0 = 0$  and thus cannot contain any terms odd in  $Q$  [Fig. 2(b)].

Collecting then the contributions larger than the cavity linewidth to the mode frequency, we have that  $\omega_{n,2} \approx \Delta_{n,2} + B_{n,2}(q - q_0)$ , and the excitation of this optical mode leads to the approximate Hamiltonian

$$H_a = H_q + \hbar\Delta_{n,2}a^\dagger a + \hbar B_{n,2}a^\dagger a q, \quad (8)$$

where  $H_q$  is the free oscillator Hamiltonian for the mechanical mode  $q$ ,  $a^\dagger$  and  $a$  are the creation and annihilation operators for the optical mode obeying  $[a, a^\dagger] = 1$ ; we have rescaled  $(q - q_0) \rightarrow q$ , and dropped  $H_Q$  the free Hamiltonian for  $Q$  since its dynamics are not affected at all. Clearly the Hamiltonian in Eq. (8) describes the backaction cooling and trapping of the breathing mode  $q$ , decoupled from the COM motion. It is achievable with parameters in the same regime as previous experiments [2–4,13].

A similar procedure can be exploited to cool and trap the mode  $Q$  only. In brief, we propose to do this by exciting  $\omega_{n,3}$  with  $q_0 = 2L$ , and  $Q_0 = 0.12\lambda_n$ , where  $\lambda_n = 4L/n$ . As can be seen from Figs. 2(b) and 2(c), around these points the optical mode depends linearly on  $Q$  and quadratically on  $q$ . Specifically for the parameters mentioned below Eq. (6), we find  $\Delta_{n,3} \sim 10^{15}$  Hz,  $B_{n,3} = P_{n,3} = 0$  [since  $\omega_{n,3}$  is even in  $q$  around  $q_0 = 2L$ ; see Fig. 2(c)],  $B'_{n,3} \sim 2\xi_{n,3}/3 = \Delta_{n,3}/3L$ , and  $M_{n,3}, M'_{n,3}$  both lead to shifts  $\sim 1$  Hz. We conclude that  $\omega_{n,3} = \Delta_{n,3} + B'_{n,3}(Q - Q_0)$ , and exciting this mode leads to a Hamiltonian analogous to Eq. (8),

$$H_b = H_Q + \hbar\Delta_{n,3}b^\dagger b + \hbar B'_{n,3}b^\dagger b Q, \quad (9)$$

which describes the backaction cooling and trapping of the mechanical mode  $Q$  by the optical mode  $b$ , decoupled from  $q$ . Equations (8) and (9) demonstrate that the modes  $q$  and  $Q$  can be independently trapped and cooled, for appropriate choices of  $q_0, Q_0$  and for cavity parameters that have already been achieved experimentally.

For the more stringent parameter  $R \leq 0.999$ , it has been suggested that QND measurements, as well as the observation of quantum jumps between membrane energy eigenstates, should be possible [13]. As  $R \rightarrow 1$ , the curves in Fig. 2

begin to resemble crossings, that is, the slopes become more linear while the extrema acquire an increasing curvature, similar to the case of a single membrane [13,14]. For the mode  $\omega_{n,2}$ , this implies that  $M_{n,2}$  becomes even smaller while  $M'_{n,2}$  can eventually make a contribution larger than the cavity linewidth and must be taken into account: for example, for  $R = 0.999$  we find  $M_{n,2}Q^2 \sim \gamma$ . Remembering that to reach the quantum mechanical ground state of vibration of the membrane(s) the system must be in the resolved-sideband regime ( $\omega_m \gg \gamma$ ) [18–20], and making the rotating-wave approximation [13], Eq. (8) can be modified to yield a Hamiltonian valid in the  $R \rightarrow 1$  regime,

$$H'_a = H_d + \hbar[\Delta_{n,2} + M'_{n,2}C_0^2c^\dagger c]a^\dagger a + \hbar B_{n,2}D_0a^\dagger a(d^\dagger + d), \quad (10)$$

where  $H_d = H_q$  and we have used creation and annihilation operators to represent the coordinates, i.e.,  $Q = C_0(c^\dagger + c)$ , with  $C_0 = (\hbar/4m\omega_m)^{1/2}$ , and  $q = D_0(d^\dagger + d)$  with  $D_0 = (\hbar/m\omega_m\sqrt{3})^{1/2}$ . This Hamiltonian indicates that the mode  $Q$  now supplies an offset to the frequency  $\omega_{n,2}$  proportional to the phonon number operator  $c^\dagger c$ . However, since  $[H'_a, c^\dagger c] = 0$ , this offset is a constant if no cooling is simultaneously performed on  $Q$ . Mode  $Q$  therefore does not influence the dynamics of mode  $q$ . Hence we have not included  $H_Q$  in  $H'_a$ . A similar modification of Eq. (9) can be made, and together with Eq. (10), this preserves our conclusions regarding independent trapping and cooling of the modes  $q$  and  $Q$ .

For the parameters proposed in Ref. [13], the frequency offsets in the modes  $\omega_{n,2}$  and  $\omega_{n,3}$  can be used to count the phonons in the mechanical COM and breathing modes, respectively. For example, the detuning of  $\omega_{n,2}$  per phonon in the  $Q$  mode is  $M'_{n,2}C_0^2 \sim \gamma$ ; see Eq. (10). Although the resolved sideband limit requires large optical detunings of the order of  $\omega_m$ , weak probe lasers can couple on resonance to  $\omega_{n,2}$  and  $\omega_{n,3}$  and monitor the detunings via a Pound-Drever-Hall measurement [13]. Since only  $Q_0$  needs to be adjusted between the cooling configurations for  $q$  and  $Q$ , a possible way to do this might be to switch off the cooling laser, translate the end mirrors of the cavity rather than the membranes themselves, and then switch on the phonon-counting laser field. Experimentally the response of the two modes  $Q$  and  $q$  can be accessed by modulating the light field at the frequencies  $\omega_m$  and  $\omega_m\sqrt{3}$ , respectively.

Before concluding we mention briefly some implications of our present work for a larger number  $N$  of membranes, a situation that may be similar to that of trapped and cooled ion chains [21,22]. We expect the optical spectrum of such a system to be similar to Fig. 2, but more complicated. Nonetheless there will be linear as well as quadratic regimes available to every mechanical mode. The optomechanical coupling parameters will be comparable to those presented here, since the amplitude of the resonator frequency variation is typically a substantial fraction of the resonator free spectral range, and the periodicity of this variation is close to the optical frequency [14].

The main challenge is then to find equilibrium points around which only the frequency of the mode to be cooled varies linearly with the corresponding normal mode coordinate, while all other modes vary quadratically. In some cases the reflection symmetry of the fixed mirrors about the origin ensures the existence of such points. It is because of this symmetry that for  $N=2$  Eq. (4) is even in  $Q$ , the COM mode. For every  $q_0$  the presence of a quadratic minimum in  $Q$  is

therefore guaranteed and  $q$  can be cooled. Similarly for  $N=3$ , with individual membrane coordinates  $q_j$  ( $j=1,2,3$ ), we expect the optical spectrum to be symmetric in the COM mode  $Q_1=(q_1+q_2+q_3)/3$  as well as in the “scissors” mode  $Q_2=(q_1-2q_2+q_3)/6$ , but not in the stretch mode  $Q_3=(q_3-q_1)/2$ . This would imply that the stretch mode  $Q_3$  can be cooled around some equilibrium point where the optical mode is certain to vary quadratically along  $Q_{1,2}$  [23].

In conclusion we have considered the extension of cavity optomechanics to multimembrane systems. We have found that the normal modes of the system can be optically cooled, trapped, and measured independently. Our work opens the way for an investigation of optomechanical cavities with a large number of membranes.

This work is supported in part by the U.S. Office of Naval Research, by the National Science Foundation, and by the U.S. Army Research Office. We thank Dr. H. Uys and O. Dutta for stimulating discussions.

- 
- [1] P. F. Cohadon, A. Heidmann, and M. Pinard, *Phys. Rev. Lett.* **83**, 3174 (1999).
- [2] D. Kleckner and D. Bouwmeester, *Nature (London)* **444**, 75 (2006).
- [3] S. Gigan *et al.*, *Nature (London)* **444**, 67 (2006).
- [4] O. Arcizet, P.-F. Cohadon, T. Briant, M. Pinard, and A. Heidmann, *Nature (London)* **444**, 71 (2006).
- [5] A. Schliesser, P. Del’Haye, N. Nooshi, K. J. Vahala, and T. J. Kippenberg, *Phys. Rev. Lett.* **97**, 243905 (2006).
- [6] T. Corbitt *et al.*, *Phys. Rev. Lett.* **98**, 150802 (2007).
- [7] W. Marshall, C. Simon, R. Penrose, and D. Bouwmeester, *Phys. Rev. Lett.* **91**, 130401 (2003).
- [8] Y. T. Yang *et al.*, *Nano Lett.* **6**, 583 (2006).
- [9] J.-M. Courty, A. Heidmann, and M. Pinard, *Phys. Rev. Lett.* **90**, 083601 (2003).
- [10] P. Treutlein, D. Hunger, S. Camerer, T. W. Hansch, and J. Reichel, *Phys. Rev. Lett.* **99**, 140403 (2007).
- [11] S. Mancini, D. Vitali, and P. Tombesi, *Phys. Rev. Lett.* **90**, 137901 (2003).
- [12] S. L. Braunstein and H.-K. Lo, *Scalable Quantum Computers: Paving the Way to Realization* (Wiley, Weinheim, 2000).
- [13] J. D. Thompson *et al.*, *Nature (London)* **452**, 72 (2008).
- [14] M. Bhattacharya, H. Uys, and P. Meystre, *Phys. Rev. A* **77**, 033819 (2008).
- [15] W. J. Fader, *IEEE J. Quantum Electron.* **21**, 1838 (1985).
- [16] D. F. V. James, *Appl. Phys. B: Lasers Opt.* **66**, 181 (1998).
- [17] D. F. V. James, *Appl. Phys. B: Lasers Opt.* **76**, 199 (2003).
- [18] I. Wilson-Rae, N. Nooshi, W. Zwerger, and T. J. Kippenberg, *Phys. Rev. Lett.* **99**, 093901 (2007).
- [19] F. Marquardt, J. P. Chen, A. A. Clerk, and S. M. Girvin, *Phys. Rev. Lett.* **99**, 093902 (2007).
- [20] A. Schliesser, R. Rivière, G. Anetsberger, O. Arcizet, and T. J. Kippenberg, *Nat. Phys.* **4**, 415 (2008); C. A. Regal, J. D. Teufel, and K. W. Lehnert, *Nat. Phys.* **4**, 555 (2008); J. D. Teufel, J. W. Harlow, C. A. Regal, and K. W. Lehnert, e-print arXiv:0807.3585.
- [21] J. I. Cirac and P. Zoller, *Phys. Rev. Lett.* **74**, 4091 (1995).
- [22] D. Wineland *et al.*, *J. Res. Natl. Inst. Stand. Technol.* **103**, 259 (1998).
- [23] M. Bhattacharya and P. Meystre (unpublished).
- [24] Estimated from the equipartition theorem  $\langle(Q-Q_0)^2\rangle^{1/2} = (k_B T/2m\omega_m^2)^{1/2}$  [13].